Sains Malaysiana 44(9)(2015): 1357–1362

Photoluminescence Characteristic of Magnesium Boro-Tellurite doped Eu^{3+} Ceramic

(Ciri Fotoluminesens bagi Magnesium Boro-Telurit dop Seramik Eu^{3+})

NUR ZU IRA BOHARI, R. HUSSIN*, ZUHAIRI IBRAHIM & HENDRIK O. LINTANG

ABSTRACT

The series samples of xTeO_2-(70-x)B_2O_3-30MgO with 0≤x≤30 mol% have been prepared via the solid-state reaction method. The composition sample of 30TeO_2-40B_2O_3-30MgO were chosen as a doped sample in the composition of 100-y(30TeO_2-40B_2O_3-30MgO)-yEu^{3+} with 0.2≤y≤2 mol% and were heated at 750°C. The XRD results showed that the major phase was $Mg(Te_2O_5)$ while $MgO(B_2O_3)_2$, $MgTe_6O_{13}$, $Mg_2(B_2O_5)$ and MgB_4O_7 was observed as a minor phase. The small phase of EuB_2O_4 and $Eu_2Te_4O_{11}$ were detected by XRD when the composition of 30TeO_2-40B_2O_3-30MgO were doped with 1.5% of Eu^{3+}. The EDX analysis of 30TeO_2-40B_2O_3-30MgO doped with 1.5% Eu^{3+} sample was confirmed the presence of boron (B), magnesium (Mg), tellurium (Te), oxygen (O) and europium (Eu) elements. From the FESEM images, the surface morphology of doped 1.5% Eu^{3+} samples was agglomerated compared with the undoped sample. The average diameter of the grain size is in the range of 50-100 µm. The emission spectra of the Eu^{3+}-doped 30TeO_2-40B_2O_3-30MgO ceramic consists of intense and sharp lines ranging from 550-725 nm. The luminescence spectra showed that the emission intensity of 30TeO_2-40B_2O_3-30MgO doped with Eu^{3+} was enhanced with the increase of Eu^{3+} ion from 0.2 to 1.5 mol%, which resulted in enhancement of the red emission of the samples. The longest decay time for 30TeO_2-40B_2O_3-30MgO doped with 1.5 mol % Eu^{3+} was 0.892 ms.

Keywords: Decay curve; magnesium boro-tellurite; photoluminescence

ABSTRAK

Siri sampel bagi xTeO_2-(70-x)B_2O_3-30MgO dengan 0≤x≤30 mol% telah disediakan melalui kaedah tindak balas keadaan pepejal. Sampel dengan komposisi 30TeO_2-40B_2O_3-30MgO telah dipilih sebagai sampel dop berkomposisi 100-y(30TeO_2-40B_2O_3-30MgO)-yEu^{3+} dengan 0.2≤y≤2 mol% dan telah dipanaskan pada suhu 750°C. Keputusan XRD menunjukkan fasa major adalah $Mg(Te_2O_5)$ manakala $MgO(B_2O_3)_2$. $MgTe_6O_{13}$, $Mg_2(B_2O_5)$ and MgB_4O_7 dilihat sebagai fasa minor. Fasa yang kecil bagi $Dy(BO_2)_3$, $Dy_2Te_4O_{11}$, EuB_2O_4 and $Eu_2Te_4O_{11}$ telah dikesan oleh XRD pada komposisi 30TeO_2-40B_2O_3-30MgO dop 1.5% Eu^{3+}. Analisis EDX bagi sampel 30TeO_2-40B_2O_3-30MgO dop 1.5% Eu^{3+} menunjukkan unsur boron (B), magnesium (Mg), telurium (Te), oksigen (O) dan europium (Eu). Daripada imej FESEM, morfologi permukaan bagi sampel dop adalah bergumpal berbanding dengan sampel tidak didop. Diameter purata bagi saiz butiran adalah dalam lingkungan 50-100 µm. Spektrum pancaran bagi Eu^{3+}-dop 30TeO_2-40B_2O_3-30MgO seramik terdiri garisan yang jelas dan tajam pada julat 550-725 nm. Spektra luminesens menunjukkan keamatan pancaran bagi 30TeO_2-40B_2O_3-30MgO dop dengan Eu^{3+} meningkat dengan peningkatan ion Eu^{3+} daripada 0.2 ke 1.5 mol%, menunjukkan peningkatan pancaran merah pada sampel tersebut. Masa pereputan yang paling lama apabila didopkan dengan 1.5 mol% Eu^{3+} pada komposisi 30TeO_2-40B_2O_3-30MgO adalah 0.892 ms.

Kata kunci: Fotoluminesens; lengkung pereputan; magnesium boro-telurit

INTRODUCTION

The high optical quality rare earth (RE) ions doped ceramics have been investigated as attractive lighting sources. Ceramics are the best host materials to incorporate high concentrations of dopant ions such as rare earth and transition metal ions besides having thermal and mechanical properties. These ceramic can be fabricated at lower cost and speedy processes in a large variety of sizes and shapes (Lupei et al. 2005; Mohr et al. 2008). Borate has been studied extensively due to the physical properties like low melting point, high thermal stability and good solubility (Elfayoumi et al. 2010). An interesting behavior of the tellurite based is good mechanical strength, chemical durability, no hygroscopic properties and low process temperature (Babu et al. 2007). Among the host materials, boro-tellurite represents favorable compromise of low phonon energy and a relatively high thermal stability, high chemical durability and ease of fabrication (Joshi et al. 2008; Yanmin et al. 2007). Rare-earth elements which act as dopant yield interesting and useful properties in host crystal. Rare-earth-doped materials also have potential applications for phosphors, display monitor, x-ray imaging and scintillators (Blasse & Grabmaier 1994). Moreover, the

luminescence properties of the ceramic could be improved by doping with rare earth (RE) ions as an activator. Eu^{3+}-doped are commonly used as red emitting materials for field emission technology and LEDs, which exhibit higher luminescence efficiency compared with other luminous materials (Oikawa & Fujihara 2005). In the present work, magnesium boro-tellurite doped Eu^{3+} ceramic with various Eu^{3+} concentration were synthesized by the solid state reaction method. The effect of Eu^{3+} dopants on the structural and luminescence characteristic are discussed.

Experimental Details

All the powder samples were synthesized by the solid state reaction method. The starting materials such as of boric acid, H_3BO_3 (99.99%), tellurium oxide, TeO_2 (99.99%), magnesium oxide, MgO (99.99%) and europium oxide, Eu_2O_3 (99.99%) were employed as the raw materials. The samples were synthesized according to the compositions of xTeO$_2$-(70-x)B$_2$O$_3$-30MgO with $0 \le x \le 30$ in appropriate amounts (mol%). The percentage of Eu_2O_3 from 0.2 to 2 mol% was then added into the mixtures. The powders were thoroughly mixed in agate mortar. The mixtures were pressed into pellets using hydraulic press with 10 ton/cm^2 pressure. After pelletized; the samples were heated at 750ºC for 6 h. The dried pellet was grounded into fine powder. The powders were prepared for the experimental measurement. The structure of the prepared powders was examined by Siemen Diffraction D5000 diffractometer with CuK_α radiation (λ = 1.54Å) and 2q scan range of 10 to 80º. The PL and lifetime measurements were performed with a Jasco Fluorescence spectrophotometer FP8500 equipped with a 150-W xenon lamp as an excitation source. The surface morphology was examined by field emission scanning electron microscope (FESEM) model SUPRA 55VP. Elemental analysis was carried out by energy dispersive X-ray (EDX) using X-ray detector attached to the FESEM instrument. All the measurements were performed at room temperature.

Results and Discussion

The XRD pattern shows the influence of varying composition of the xTeO$_2$-(70-x)B$_2$O$_3$-30MgO with $0 \le x \le 30$ mol%. It can be observed that all the diffraction peaks in XRD patterns assigned to Mg(Te$_2$O$_5$), MgO(B$_2$O$_3$)$_2$, MgTe$_6$O$_{13}$, Mg$_2$(B$_2$O$_5$) and MgB$_4$O$_7$, which were well matches with the JCPDS No. 01-073-3922, 01-076-0666, 00-028-0634, 01-086-0531 and 00-031-0787, respectively. Figure 1 shows the intensity of the peaks increases with increasing x mol% and the phases appear clearly at x = 30 mol%. From the XRD results, the major peaks due to Mg(Te$_2$O$_5$) can be observed followed by MgO(B$_2$O$_3$)$_2$. MgTe$_6$O$_{13}$, Mg$_2$(B$_2$O$_5$) and MgB$_4$O$_7$ also was observed as a minor peaks. The XRD patterns of 30TeO$_2$-40B$_2$O$_3$-30MgO doped with 1.5% of Eu^{3+} is shown in Figure 2. The pattern shows that a small amount of rare earth ions also can be observed as a minor phase. With the addition of dopant into the sample, the peaks of EuB$_2$O$_4$ and Eu$_2$Te$_4$O$_{11}$ were included into the XRD pattern. The previous results also showed that rare earth ions phase can be detected (Cheng et al. 2014; Kumar & Buddhuda 2009; Kunimoto et al. 2013).

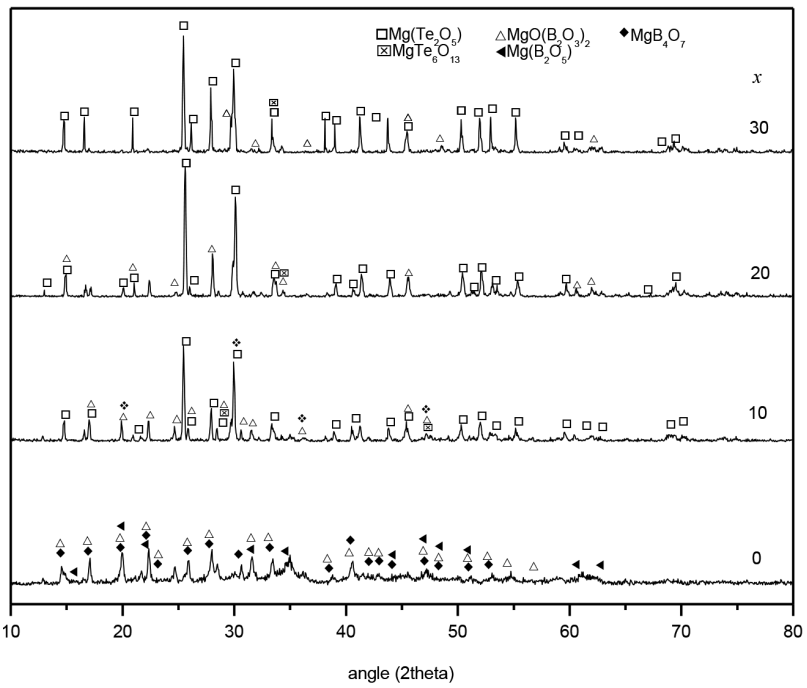

FIGURE 1. X-ray diffraction pattern of xTeO$_2$-(70-x)B$_2$O$_3$-30MgO with $0 \le x \le 30$ mol% ceramic sample prepared at 750ºC

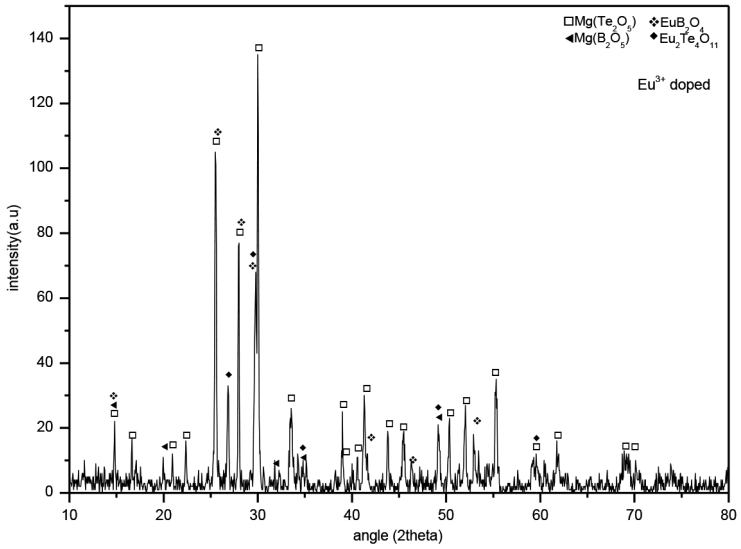

FIGURE 2. X-ray diffraction pattern of $30TeO_2$-$40B_2O_3$-30MgO doped 1.5% of Eu^{3+} ceramic sample prepared at 750°C

EDX analysis was carried out to confirm the presence of rare earth ion in the samples. Figure 3 shows the EDX spectra of $30TeO_2$-$40B_2O_3$-30MgO doped 1.5% of Eu^{3+}. The EDX analysis confirmed the presence of boron (B), magnesium (Mg), tellurium (Te) and oxygen (O) and europium (Eu) elements. Figure 4 shows the FESEM images of $30TeO_2$-$40B_2O_3$-30MgO doped 1.5% of Eu^{3+} at 750°C. The doped sample has different morphological structures and grain size compared with the undoped sample. The structure of the doped samples is more agglomerated compared with the undoped sample. The samples have an average grain size of 50-100 μm.

The excitation spectra of 100-y($30TeO_2$-$40B_2O_3$-30MgO)-$y$$Eu^{3+}$ ceramic with $0.2 \leq y \leq 2$ mol% at 750°C monitored at 615.68 nm emission are given in Figure 5. The broad band from 200 to 350 nm is attributable to the charge transfer band (CTB) transition. The CTB plays an important role in its luminescence. The broad absorption band is assigned to the CTB of Eu-O (Sun & Fu 2012), which occurred by electronic transition from the filled 2p orbital of O^{2-} to the partially filled 4f orbital of Eu^{3+}. The CTB is related closely to the covalency between O^{2-} and Eu^{3+} and the coordination environment around Eu^{3+} (Tian et al. 2009). It has been reported that CTB in oxides due to Eu^{3+}- O^{2-} interaction might arise (Rao et al. 2008). The sharp lines 363.01 nm ($^7F_0$-$^5D_4$), 382.86 nm ($^7F_0$-$^5G_3$), 396.61 nm ($^7F_0$-$^5L_6$), 417.14 nm ($^7F_0$-$^5D_3$), 428.74 nm ($^7F_0$-$^5D_3$), 451.43 nm ($^7F_0$-$^5D_2$), 465.78 nm ($^7F_0$-$^5D_2$), 474.72 nm ($^7F_0$-$^5D_2$), 489.07 nm ($^7F_0$-$^5D_2$), 517.16 nm ($^7F_0$-$^5D_1$), 527.48 nm ($^7F_0$-$^5D_1$) and 537.07 nm ($^7F_0$-$^5D_1$) were observed,

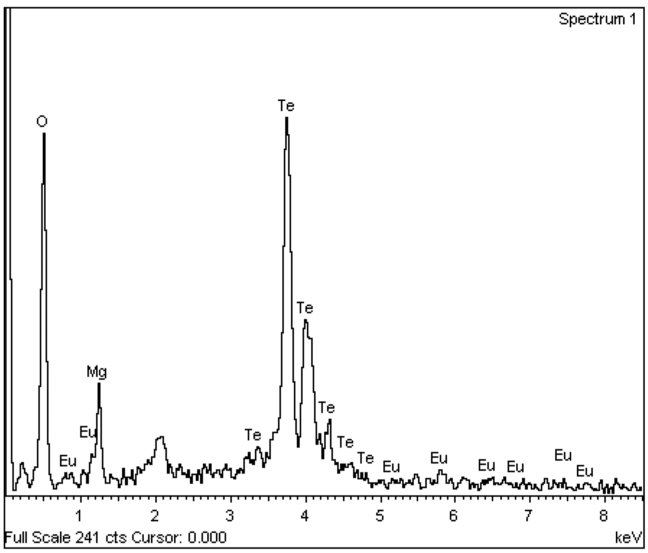

FIGURE 3. EDX spectrum of $30TeO_2$-$40B_2O_3$-30MgO doped 1.5% of Eu^{3+} ceramic sample prepared at 750°C

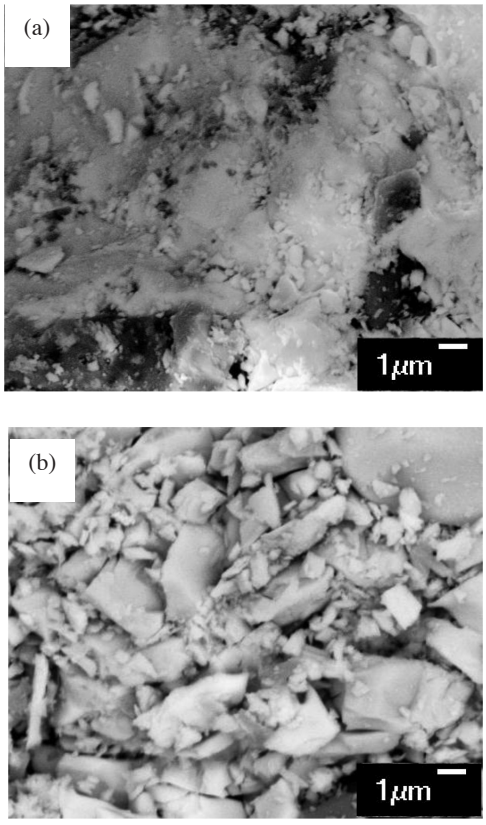

FIGURE 4. FESEM images of $30TeO_2$-$40B_2O_3$-30MgO (a) x =30 (b) 1.5% of Eu^{3+} ceramic sample prepared at 750°C (magnification: 10K ×)

respectively. The adsorbed spectra showed that when the wavelength ranged from 350-550 nm, the sharp peaks originated from the transitions with the *f*-configuration from $^7F_0$ to the excitation states (Visser et al. 1992). No significant shift in peak position was observed for the various Eu^{3+} ion concentrations. The $^7F_0$ to $^5G_3$ at 382.86 nm and $^7F_0$-$^5L_6$ transition at 396.61 nm were the two strongest absorptions. The prominent excitation band at 396.61 nm has been chosen for the measurement of emission spectra of $30TeO_2$-$40B_2O_3$-30MgO doped Eu^{3+} ceramic. However, the intensities of the peaks in the excitation spectra increased in order of 0.2, 0.4, 0.6, 0.8, 1.0, 1.5 and 2 mol%. As the Eu^{3+} ion concentration increases, the CTB of Eu-O also increases and is shifted towards the shorter wavelength (higher energy) region.

The luminescence spectrum of $30TeO_2$-$40B_2O_3$-30MgO doped Eu^{3+} (Eu^{3+} = 0.2, 0.4, 0.6, 0.8, 1.0, 1.5 and 2 mol%) ceramic obtained by excitation of Eu^{3+} at 396.61 nm are displayed in Figure 6. It can be seen that the emission spectra of the Eu^{3+}-doped $30TeO_2$-$40B_2O_3$-30MgO ceramic is composed of intense and sharp lines ranging from 550-725 nm, which are related to transition from the excited $^5D_0$ level to ^7F_J (J=0-4) levels (Li et al. 2012). The strong emission peaks observed at 593.21, 615.68 and 701.20 nm were assigned to the transitions of $^5D_0$-$^7F_1$, $^5D_0$-$^7F_2$, and $^5D_0$-$^7F_4$. Besides, the weak emission was observed at 642.14 and 654.08 nm ascribed to the transition of $^5D_0$-$^7F_3$. Among these peaks, the red emission peak at 615.68 nm is more dominant than the other peaks. This peak originates from the electric dipole transitions of $^5D_0$-$^7F_2$, which indicates that Eu^{3+} occupies a non-centro-symmetric site (Meng et al. 2012). The luminescence spectra showed that the emission intensity of $30TeO_2$-$40B_2O_3$-30MgO doped with Eu^{3+} was enhanced with the increase of Eu^{3+} ion concentration from 0.2 to 1.5 mol%, which resulted in enhancement of the red emission of the samples. When the Eu^{3+} ion concentration continuously increase to 2 mol%, the emission intensity decreases because of the concentration quenching effect. With the increase of Eu^{3+} concentration, the proportion of non-radiative energy transfer between nearby Eu^{3+} ions exceeds the critical value and the luminescence intensity begins to decrease (Cui et al. 2013).

Figure 7 shows the measured fluorescence decay curve of the $30TeO_2$-$40B_2O_3$-30MgO doped Eu^{3+} ceramic for various Eu^{3+} concentrations. With the increase of Eu^{3+}

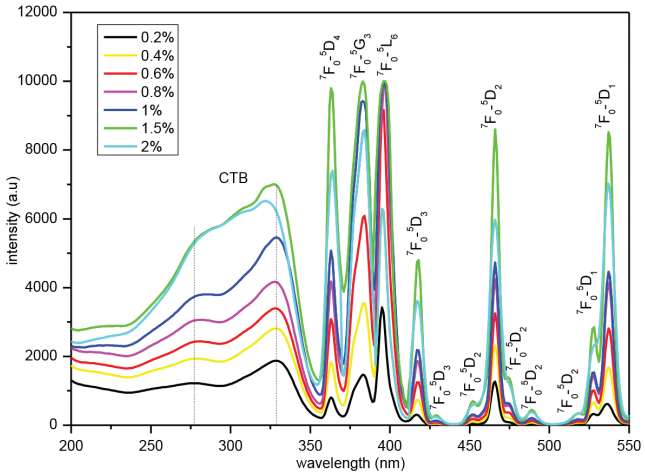

FIGURE 5. Excitation spectra of 100-x($30TeO_2$-$40B_2O_3$-30MgO)-$x$$Eu^{3+}$ with 0.2≤x≤2 mol% ceramic sample prepared at 750°C

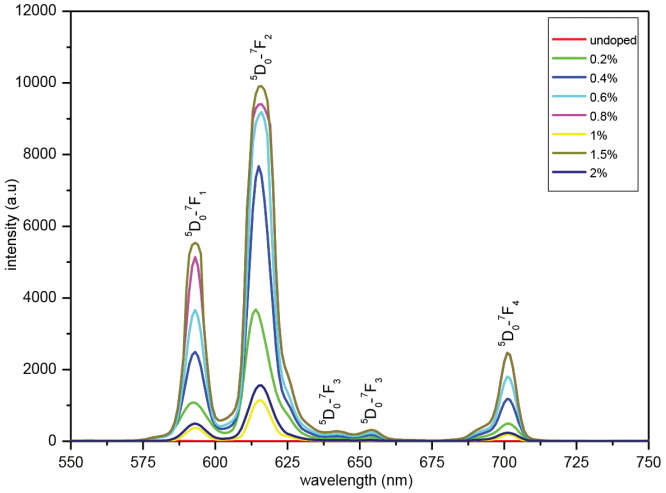

FIGURE 6. Emission spectra of 100-x(30TeO_2-40B_2O_3-30MgO)-$x$$Eu^{3+}$ with 0.2≤x≤2 mol% ceramic sample prepared at 750°C

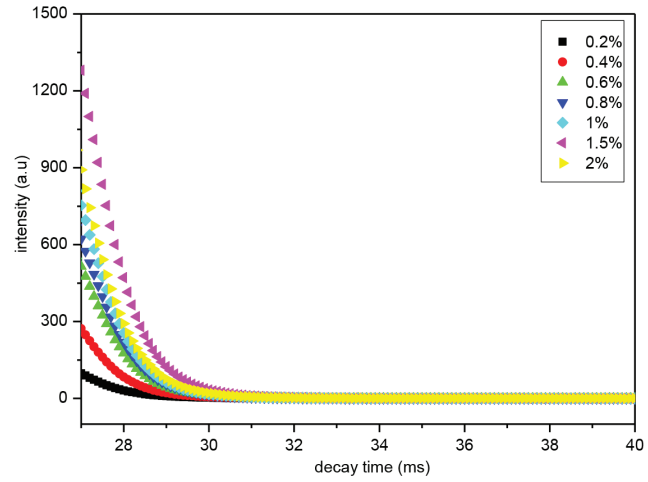

FIGURE 7. Lifetime spectra of 100-x(30TeO_2-40B_2O_3-30MgO)-$x$$Eu^{3+}$ with 0.2≤x≤2 mol% ceramic sample prepared at 750°C

concentrations from 0.2 to 1.5 mol%, the decay time value of Eu^{3+} ion increased from 0.834 ms to 0.892 ms and decrease to 0.846 ms at 2 mol%. The longest decay time occurred at 1.5 mol% of Eu^{3+}. The sample doped with 2 mol% Eu^{3+} had reached a concentration quenching effect and caused shorter lifetime (Fang et al. 2006). The decay curves of 30TeO_2-40B_2O_3-30MgO doped Eu^{3+} ceramic values with the various concentrations of Eu^{3+} ions were listed as shown in Table 1.

TABLE 1. Decay times for 100-x(30TeO_2-40B_2O_3-30MgO)-$x$$Eu^{3+}$ with 0.2≤x≤2 mol% ceramic sample prepared at 750°C

Concentration of Eu^{3+} (mol %)	Decay time (ms)
0.2	0.834
0.4	0.853
0.6	0.858
0.8	0.860
1.0	0.866
1.5	0.892
2.0	0.846

CONCLUSION

In summary, the samples of magnesium boro-tellurite and magnesium boro-tellurite doped Eu^{3+} ceramic have been prepared using the solid-state reaction method. From the XRD profiles, the major peaks due to Mg(Te_2O_5) was observed in each profile followed by $MgO(B_2O_3)_2$, $MgTe_6O_{13}$, $Mg_2(B_2O_5)$ and MgB_4O_7 observed as weak peaks. The peaks of EuB_2O_4 and $Eu_2Te_4O_{11}$ were included into the XRD patterns of 30TeO_2-40B_2O_3-30MgO doped 1.5% of Eu^{3+}. The morphology of the ceramic studied using the SEM images shows that the particles are agglomerated and the particles are in micron size. From the luminescence

study, the emission intensity of the 615.68 nm increases rapidly with Eu^{3+} concentration up to 1.5 mol%. When the Eu^{3+} concentration is above 1.5 mol%, concentration quenching occurred. The highest value of the decay time was obtained at 1.5 mol% of Eu^{3+}. Based on the results of emission spectral, we suggest that these ceramic powders are brightly luminescent and are applicable as novel optical materials.

ACKNOWLEDGEMENTS

The authors would like to thank the Fundamental Research Grant Scheme (FRGS) under research grant Project Number: Q.J130000.2526.03H97 for the financial support. We would also like to thank the Faculty of Science, Universiti Teknologi Malaysia (UTM) and Institute of Ibnu Sina for the facilities provided.

REFERENCES

Babu, P., Seo, H.J., Jang, K.H., Kumar, K.U. & Jayasankar, C.K. 2007. Optical spectroscopy, 1.5 μm emission, and upconversion properties of Er^{3+}-doped metaphosphate laser glasses. *Journal of the Optical Society of America B* 24(9): 2218-2228.

Blasse, G. & Grabmaier, B.C. 1994. *Luminescence Materials*. Berlin: Springer-Verlag.

Cheng, L.Y., Dan, P.G., Fei, W., Ming, Y.Z., Ai, L.Z., Xiao, Y.L., Ying, X.L., Xin, Y.L., Hai, B.B. & Yu, L.P. 2014. On the luminescent properties of Dy^{3+}:β-Li_2TiO_3 omment on 'Synthesis and emission analysis of RE^{3+} (Eu^{3+} or Dy^{3+}): Li_2TiO_3 ceramics'. *Ceramics International* 40: 11465-11467.

Cui, R., Deng, C., Gong, X., Li, X. & Zhou, J. 2013. Luminescent performance of rare earths doped $CaBi_2Ta_2O_9$ phosphor. *Journal of Rare Earths* 31(6): 546-550.

Elfayoumi, M.A.K., Farouk, M., Brik, M.G. & Elokr, M.M. 2010. Spectroscopic studies of Sm^{3+} and Eu^{3+} co-doped lithium borate glass. *J. Alloys Compd*. 492(1-2): 712-716.

Fang, T.H., Hsiao, Y.J., Chang, Y.S. & Chang, Y.H. 2006. Photoluminescent characterization of $KNbO_3$:Eu^{3+}. *Materials Chemistry and Physics* 100: 418-422.

Joshi, P., Shen, S. & Jha, A. 2008. Er^{3+}-doped boro-tellurite glass for optical amplification in the 1530-1580 nm. *Journal of Appl. Phys*. 103(8): 083543.

Kumar, G.B. & Buddhudu, S. 2009. Synthesis and emission analysis of RE^{3+} (Eu^{3+} or Dy^{3+}): Li_2TiO_3 ceramics. *Ceramics International* 35: 521-525.

Kunimoto, T., Honma, T., Ohmi, K., Okubo, S. & Ohta, H. 2013. Detailed impurity phase investigation by X-ray absorption fine structure and electron spin resonance analyses in synthesis of $CaMgSi_2O_6$: eu phosphor. *Japanese Journal of Applied Physics* 52: 042402.

Li, S., Xu, D., Shen, H., Zhou, J. & Fan, Y. 2012. Synthesis and Raman properties of magnesium borate micro/nanorods. *Materials Research Bulletin* 47: 3650-3653.

Lupei, V., Lupei, A. & Ikesue, A. 2005. Transparent Nd and (Nd, Yb)-doped Sc_2O_3 ceramics as potential new laser materials. *Appl. Phys. Lett*. 86: 111-118.

Meng, F.G., Zhang, X.M., Li, H. & Seo, H.J. 2012. Synthesis and spectral characteristics of La_2MoO_6: Ln^{3+} (Ln=Eu, Sm, Dy, Pr, Tb) polycrystals. *J. Rare Earths* 30(9): 866-870.

Mohr, D., Andrea, S.S., Camargo, D., Schneider, J.F., Quieroz, T.B., Eckert, H., Botero, E.R., Garcia, D. & Eiras, J.A. 2008. Solid state NMR as a new approach for the structural characterization of rare earth doped lead lanthanum Zirconate titanate laser ceramics. *Solid State Sci*. 10: 1401-1407.

Oikawa, M. & Fujihara, S. 2005. Sol-gel preparation and luminescence properties of CeO_2: Ln (Ln = Eu^{3+} and Sm^{3+}) thin films. *Journal of European Ceramic Society* 25: 2921-2924.

Rao, B.V., Rambabu, U. & Buddhudu, S. 2008. Photoluminescence spectral analysis of Eu^{3+}: Phosphors. *Physica B* 382: 86-91.

Sun, Y.H. & Fu, Y.X. 2012. Synthesis and characteristics of nano-size sandwich structure (Y,Gd)BO_3: Eu^{3+} phosphors. *J. Luminescence* 132: 550-557.

Tian, Y., Qi, X., Wu, X., Hu, R. & Chen, B. 2009. Luminescent properties of $Y_2(MoO_4)_3$:Eu^{3+} red phosphors with flowerlike shape prepared via co-precipitation method. *J. Phys. Chem. C* 113: 10767-10772.

Visser, O., Visscher, L., Aerts, P.J.C. & Nieuwpoort, W.C. 1992. Molecular open shell configuration interaction calculations using the Dirac-Coulomb Hamiltonian: The f^6 manifold of an embedded EuO_6^{9-} cluster. *J. Chem. Phys*. 96(4): 2910.

Yanmin, Y., Baojiu, C., Cheng, W., Guozhong, R. & Xiaojun, W. 2007. Investigation of modification effect of B_2O_3 component on optical spectroscopy of Er^3+ doped tellurite glasses. *J. Rare Earths* 25(1): 31-35.

Nur Zu Ira Bohari, Rosli Hussin* & Zuhairi Ibrahim
Phosphor Research Group, Department of Physics
Faculty of Science, University Teknologi Malaysia
81310 Skudai, Johor Darul Takzim
Malaysia

Hendrik O. Lintang
Ibnu Sina Institute for Fundamental Science Studies
81310 Skudai, Johor Darul Takzim
Malaysia

*Corresponding author; email: roslihussin@utm.my

Received: 23 October 2014
Accepted: 5 May 2015